Michigan
Version: 1.0.00
Released: 2026-04-09

Simulation of Cancer Outcomes and Policy Evaluation (SCOPE): Model Profile

University of Michigan

Contact

Krithika Suresh (ksuresh@umich.edu)

Funding

The development of this model was partially supported by the NIH/NCI CISNET Prostate Cancer Grant (U01CA253915) with additional funding from the Univeristy of Michigan Rogel Cancer Center and the American Cancer Society.

Suggested Citation

Suresh K, Taylor JMG, Tsodikov, A. Simulation of Cancer Outcomes and Policy Evaluation (SCOPE): Model Profile. [Internet] Apr 9, 2026. Cancer Intervention and Surveillance Modeling Network (CISNET). Available from: https://cisnet.cancer.gov/resources/files/mpd/prostate/CISNET-prostate-scope-umich-model-profile-1.0.00-2026-04-09.pdf

Version Table

Version	Date	Notes
1.0.00	2026-04-09	Initial version of model profile

Michigan
Readers Guide

Reader's Guide

Core Profile Documentation

These topics will provide an overview of the model without the burden of detail. Each can be read in about 5-10 minutes. Each contains links to more detailed information if required.

Model Purpose
This document describes the primary purpose of the model.

Model Overview
This document describes the primary aims and general purposes of this modeling effort.

Assumption Overview
An overview of the basic assumptions inherent in this model.

Parameter Overview
Describes the basic parameter set used to inform the model, more detailed information is available for each specific parameter.

Component Overview
A description of the basic computational building blocks (components) of the model.

Output Overview
Definitons and methodologies for the basic model outputs.

Results Overview
A guide to the results obtained from the model.

Key References
A list of references used in the development of the model.

Further Reading

These topics will provide a intermediate level view of the model. Consider these documents if you are interested in gaining a working knowledge of the model, its inputs and outputs.

Model Purpose

Model Purpose

Summary

The University of Michigan Simulation of Cancer Outcomes and Policy Evaluation (SCOPE) model is a stochastic, individual-level model of prostate cancer natural history that integrates PSA dynamics, disease onset and progression, screening, diagnostic pathways, treatment, and disease-specific and other-cause mortality. The model is structured around an underlying latent disease process that drives post-onset PSA trajectories, disease progression, and clinical diagnosis. It is designed to evaluate risk-adaptive screening and treatment strategies to inform clinical and policy decision-making.

Purpose

The SCOPE model preserves key components of the University of Michigan Self-Consistency Analysis of Surveillance (SCANS) analytic model while extending the representation of preclinical disease through longitudinal PSA dynamics and an underlying latent tumor growth process.

The SCANS model is an analytic model of prostate cancer incidence, diagnosis, treatment, and survival comprised of three components.[1]

(1) A model for age at disease onset and age at clinical diagnosis, where the interval between these events defines the sojourn time. Onset age for each person is defined as the youngest age at which prostate cancer could potentially be detected by a biopsy. Screening based on PSA tests can lead to earlier, screen-detected diagnosis, with advancement in time relative to clinical diagnosis defined as the lead time.
(2) A model for disease characteristics at diagnosis (stage and grade), specified using a multinomial framework that depends on mode of detection and lead time.[2,3]
(3) A model for post-diagnosis treatment and survival, conditional on stage, grade, and lead time.

The SCANS model was estimated based on maximum likelihood and algorithms specifically developed to make the comprehensive joint model tractable using population-based incidence and survival data from SEER.[4,5]It has been used to study prostate cancer trends and screening outcomes.[6-9]

SCOPE preserves the SCANS formulations for age at onset and post-diagnosis survival and is calibrated to reproduce key SCANS targets, including the distribution of sojourn times and the joint distribution of stage and grade at diagnosis. However, rather than representing preclinical disease implicitly, SCOPE introduces an explicit latent tumor growth process that generates longitudinal PSA trajectories, disease progression, and clinical detection at the individual level. This framework allows representation of longitudinal biomarkers, dynamic screening decisions, and individual disease trajectories while maintaining consistency with the established SCANS framework.

The model can be used to evaluate comparative effectiveness and cost-effectiveness of prostate cancer screening and treatment strategies, including risk-based approaches that tailor screening intervals, biopsy decisions, and stopping ages based on individual risk profiles. By incorporating an underlying latent tumor growth process, the model provides a unified framework in which longitudinal PSA trajectories, stage progression, grade progression, and clinical detection arise from a common underlying disease process. The current implementation allows diagnostic test performance to depend on disease characteristics such as grade and provides a flexible platform for evaluating dynamic, personalized screening and diagnostic pathways.

References

1. Tsodikov A, Szabo A, Wegelin J. A population model of prostate cancer incidence. Statistics in Medicine. Wiley Online Library; 2006;25(16):2846–2866.

2. Tsodikov A, Chefo S. Generalized self-consistency: Multinomial logit model and Poisson likelihood. Journal of statistical planning and inference. Elsevier; 2008;138(8):2380–2397.
3. Chefo S, Tsodikov A. Stage-specific cancer incidence: An artificially mixed multinomial logit model. Statistics in medicine. Wiley Online Library; 2009;28(15):2054–2076.
4. Wang S, Tsodikov A. A self-consistency approach to multinomial logit model with random effects. Journal of statistical planning and inference. Elsevier; 2010;140(7):1939–1947.
5. Tsodikov A, Liu LX, Tseng C. Likelihood transformations and artificial mixtures. Statistical Modeling for Biological Systems: In Memory of Andrei Yakovlev. Springer; 2020. p. 191–209.
6. Tsodikov A, Gulati R, Heijnsdijk EA, Pinsky PF, Moss SM, Qiu S, De Carvalho TM, Hugosson J, Berg CD, Auvinen A, others. Reconciling the effects of screening on prostate cancer mortality in the ERSPC and PLCO trials. Annals of internal medicine. American College of Physicians; 2017;167(7):449–455.
7. Tsodikov A, Gulati R, de Carvalho TM, Heijnsdijk EA, Hunter-Merrill RA, Mariotto AB, de Koning HJ, Etzioni R. Is prostate cancer different in black men? Answers from 3 natural history models. Cancer. Wiley Online Library; 2017;123(12):2312–2319.
8. Gulati R, Tsodikov A, Etzioni R, Hunter-Merrill RA, Gore JL, Mariotto AB, Cooperberg MR. Expected population impacts of discontinued prostate-specific antigen screening. Cancer. Wiley Online Library; 2014;120(22):3519–3526.
9. Etzioni R, Tsodikov A, Mariotto A, Szabo A, Falcon S, Wegelin J, Ditommaso D, Karnofski K, Gulati R, Penson DF, others. Quantifying the role of PSA screening in the US prostate cancer mortality decline. Cancer Causes & Control. Springer; 2008;19(2):175–181.

Model Overview

Model Overview

Summary

This document describes the structure of the Simulation of Cancer Outcomes and Policy Evaluation (SCOPE) prostate cancer microsimulation model, its relationship to the legacy University of Michigan Self-Consistency Analysis of Surveillance (SCANS) analytic model, and the extensions introduced to incorporate longitudinal PSA dynamics and disease progression for the evaluation of screening and treatment strategies.

Background

The University of Michigan SCANS model provides a tractable analytic framework for prostate cancer natural history, diagnosis, and survival; however, it does not explicitly represent longitudinal PSA trajectories or underlying disease progression. This limits its ability to incorporate emerging data sources such as MRI and biomarkers and to evaluate adaptive, risk-based screening strategies that depend on evolving patient information. These limitations motivated the development of a microsimulation model that preserves the structure and calibration targets of the analytic model while introducing a more flexible representation of disease and observation processes.

Model Description

The SCOPE microsimulation model extends the SCANS analytic framework to a stochastic, individual-level representation of prostate cancer natural history, screening, diagnosis, and treatment. The SCOPE model specifies the preclinical disease component using a latent tumor growth framework that drives longitudinal post-onset PSA trajectories, disease progression, and clinical detection. The preclinical component is calibrated to reproduce key targets from the SCANS model, including the distribution of sojourn times and the joint distribution of stage and grade at diagnosis.

The SCOPE model keeps the SCANS formulation for age at onset, which follows a Weibull distribution beginning at age 40. Following onset, each individual is assigned a latent tumor growth trajectory, with tumor extent evolving over time according to an exponential growth model with subject-specific rates. This latent tumor extent serves as a central driver of post-onset PSA dynamics, disease progression, and clinical detection.

Observed PSA values are modeled on the log scale as the sum of a non-cancer component and a cancer-related component, along with measurement error. The non-cancer component is specified using a random intercept and slope mixed-effects model, while the cancer-related component is proportional to tumor extent. This formulation enables realistic PSA trajectories both before and after cancer onset.

Disease progression is represented through stage and grade processes that evolve over time as functions of tumor extent. Stage is modeled as a transition from local disease at onset to regional and then distant disease, with transition hazards depending on tumor extent. Grade is modeled using three categories (Gleason 2-6, 7, 8-10), with transitions between categories governed by tumor extent-dependent hazards. The distribution of stage and grade at clinical diagnosis is calibrated to the predictions from the SCANS model. Clinical detection is modeled using a hazard function following onset, with the hazard depending on tumor extent and parameterized to maintain consistency with the sojourn time distribution in the SCANS model.

PSA screening is applied according to specified policies, with observed PSA values determining subsequent actions such as biopsy or additional testing, as well as potentially modifying the timing of future screening.

Secondary diagnostic tests, including MRI and biomarkers, are modeled as binary outcomes. In the current implementation, MRI sensitivity depends on disease grade and the selected positivity threshold, while biopsy sensitivity depends on disease grade and biopsy approach. The framework is sufficiently flexible to

accommodate future extensions in which test performance depends on additional disease characteristics, biomarkers, or latent tumor features.

Post-diagnosis survival is modeled from the time of clinical detection, using survival curves that depend on treatment, stage, and grade at diagnosis. Prostate cancer death is not allowed prior to clinical detection. Individuals diagnosed with low-risk disease may enter active surveillance, with surveillance protocols explicitly modeled and transitions to treatment occurring upon disease progression or clinical detection. Other-cause mortality is modeled based on U.S. life tables as a function of age and birth cohort.

By incorporating an underlying latent disease process, the model supports coherent integration of longitudinal PSA and disease progression and, in future extensions, can allow test performance to vary with tumor characteristics and growth. This enables evaluation of dynamic, personalized screening and diagnostic pathways and provides a flexible platform for incorporating emerging biomarkers and diagnostic technologies.

Assumption Overview

Assumption Overview

Summary

This document describes the assumptions underlying the University of Michigan prostate cancer microsimulation model, including assumptions about tumor growth, PSA dynamics, disease progression, and clinical detection. Where appropriate, mathematical formulations corresponding to these assumptions are provided.

Background

The University of Michigan microsimulation model is built upon the SCANS analytic framework but extends it by introducing a latent tumor growth process that drives PSA dynamics, disease progression, and detection. In contrast to models that directly link PSA to disease progression, this formulation assumes that both PSA and disease progression arise from an underlying latent tumor extent. This approach enables a coherent and mechanistic representation of longitudinal biomarkers and disease processes, while preserving consistency with the calibration targets of the SCANS model.

Assumption Listing

Tumor Onset

We assume that the age at onset of preclinical prostate cancer follows a Weibull distribution beginning at age 40. The survival function for remaining free of onset is given by:

$$S(a) = \exp\left\{-\left(\frac{1}{\mu_O}\right)^{s_O} \log(2)(a-40)^{s_O}\right\}$$

where μ_O and s_O are scale and shape parameters chosen to match the onset distribution used by the SCANS model. Figure 1 shows the probability of remaining free of prostate cancer onset by age and race.

Figure 1. Probability of remaining free of prostate cancer onset by age and race.

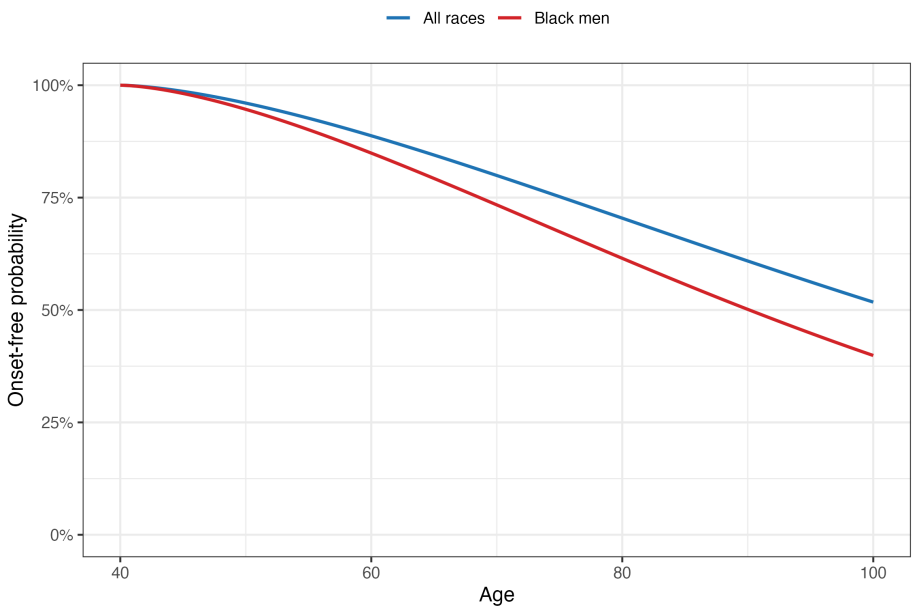

Tumor Growth

Following disease onset at age y_i, tumor extent evolves according to an exponential growth model:

$$V_i(a|y_i) = R \cdot \exp\{\gamma_i(a - y_i)\},$$

where $\gamma_i \sim \text{Gamma}(\alpha_E, \theta_E)$ represents subject-specific growth rates. Tumor extent is a latent quantity that drives PSA, disease progression, and detection.

PSA Dynamics

Observed PSA is modeled on the logarithmic scale as the combination of a non-cancer component and a cancer-related component:

$$\log(PSA_i(a)) = \log(PSA_i^{nc}(a) + PSA_i^c(a)) + \epsilon_i(a),$$

where

$$\log(PSA_i^{nc}(a)) = b_{0i} + b_{1i}(a - 35), \quad PSA_i^c(a) = \delta V_i(a|y_i),$$

and

- $\beta_{0i} \sim \mathcal{N}(\mu_0, \sigma_0^2)$
- $\beta_{1i} \sim \mathcal{N}(\mu_1, \sigma_1^2) I(\beta_{1i} > 0)$ represents a truncated normal distribution to prevent negative mean PSA growth with age
- $\epsilon_i(a) \sim \mathcal{N}(0, \sigma_P^2)$
- $I(\cdot)$ is the usual indicator function (i.e., $I(A) = 1$ if A is true and $I(A) = 0$ otherwise)

PSA levels are assumed to arise from the combination of a non-cancer component and a cancer-related component. The non-cancer component follows a linear trajectory on the logarithmic scale with age, with subject-specific intercepts and slopes. After cancer onset, tumor extent increases exponentially over time according to a subject-specific growth rate, and the cancer-related PSA component is assumed to be proportional to tumor extent. As a result, total PSA exhibits accelerated growth after onset, reflecting the contribution of tumor-driven PSA. PSA trajectories vary across individuals due to heterogeneity in baseline PSA levels, age-related growth, and tumor growth rates, and measurements are subject to normally distributed error over time. In Figure 2, we demonstrate the median PSA growth trajectories and interquartile ranges before and after onset by Gleason grade at clinical diagnosis.

Figure 2. Simulated longitudinal PSA trajectories for four individuals under the natural history model in the absence of PSA screening. Blue lines represent annual PSA values over age on a logarithmic scale. Vertical dashed lines indicate the simulated age of latent prostate cancer onset. Open triangles denote clinical diagnosis, and asterisks denote prostate cancer death.

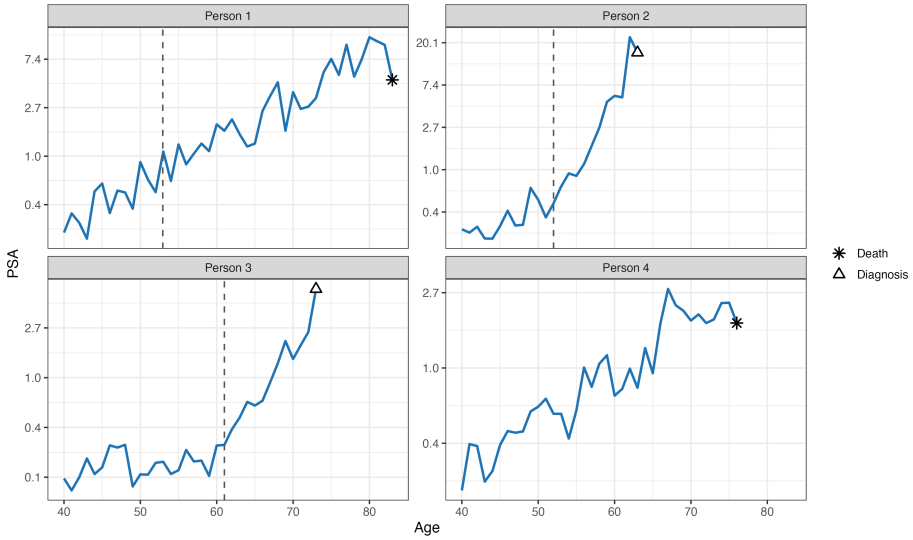

Stage Progression

All individuals begin in a localized stage at onset. We define transitioning to regional and distant stages using stage-specific hazards:

$$S_{1,\text{stage}}(a) = \exp\left\{-\frac{\beta_{1S}}{s_S}\gamma_i^{s_S-1}(a-y)^{s_S}\right\}$$

$$S_{2,\text{stage}}(a) = I(a > a_s)\exp\left\{-\frac{\beta_{2S}}{s_S}\gamma_i^{s_S-1}\left[(a-y)^{s_S} - (a_s-y)^{s_S}\right]\right\}$$

where a_s is the age at which an individual transitions from localized to regional stage, and y is age at onset.

This assumption implies that the probability of progression increases with tumor growth and faster-growing tumors progress more rapidly through stage states. Figure 3 shows the probabilities of being in each stage from time of prostate cancer onset.

Grade Progression

All individuals begin with Gleason grade 2-6. We define transitions to Gleason 7 and 8-10 as:

$$S_{1,\text{grade}}(a) = \exp\left\{-\frac{\beta_{1G}}{s_G}\gamma_i^{s_G-1}(a-y)^{s_G}\right\}$$

$$S_{2,\text{grade}}(a) = I(a > a_g)\exp\left\{-\frac{\beta_{2G}}{s_G}\gamma_i^{s_G-1}\left[(a-y)^{s_G} - (a_g-y)^{s_G}\right]\right\}$$

where a_g is the age of transition from Gleason grade 2-6 to 7, and y is age at onset.

This assumption implies that grade progression is driven by underlying tumor growth and faster-growing tumors progress more rapidly through grade states. Figure 3 shows the probabilities of being in each Gleason grade group from time of prostate cancer onset.

Figure 3. Estimated stage-state and grade-state probabilities over time since latent prostate cancer onset in a simulated cohort generated from the microsimulation model. The left panel shows the probability of being in each disease stage (localized, regional, or distant), and the right panel shows the probability of being in each Gleason grade category (Gleason 2–6, 7, or 8–10) as a function of years since onset. Probabilities were calculated among simulated individuals with latent onset who remained alive and under follow-up at each time point and normalized to sum to one at each duration since onset.

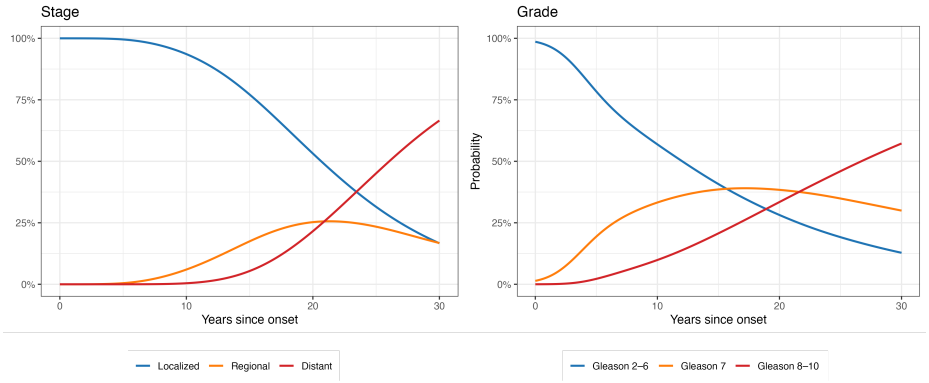

Clinical Detection

Clinical diagnosis occurs according to a hazard function that depends on tumor extent:

$$h_{CD}(a|y_i) = \beta_{CD}\gamma_i^{s_{CD}-1}(a-y_i)^{s_{CD}-1}.$$

where β_{CD} is derived from the analytic representation of the SCANS model that uses a Weibull hazard with median μ_{ACD} and shape s_{ACD} as

$$\beta_{CD} = \frac{\Gamma(\alpha_E)\theta_E^{s_{CD}-1}}{\Gamma(\alpha_E + s_{CD} - 1)} \cdot \left(\frac{1}{\mu_{ACD}}\right)^{s_{ACD}} s_{ACD} \log(2) \exp\left\{-0.1392 I(a < 68) + 0.1890 I(a > 75)\right\}$$

The corresponding survival function is:

$$S_{CD}(a) = \exp\left\{-\frac{\beta_{CD}}{s_{CD}} \gamma_i^{s_{CD}-1} (a - y_i)^{s_{CD}}\right\}.$$

The μ_{ACD} and s_{ACD} parameters are fixed to estimates derived from the SCANS model fit to SEER data. Calibration is performed to reproduce the sojourn time distribution implied by the SCANS model while allowing detection risk to vary according to latent tumor growth. Figure 4 shows the simulated distributions of age at prostate cancer onset and age at clinical diagnosis in the absence of screening.

Figure 4. Distributions of age at latent prostate cancer onset and age at clinical diagnosis in the absence of screening for a cohort simulated using the microsimulation model. Density curves summarize the distribution of ages at latent onset (blue) and subsequent clinical diagnosis (red) among individuals who developed prostate cancer. The rightward shift of the clinical diagnosis distribution relative to onset reflects the simulated preclinical sojourn time between disease onset and clinical detection.

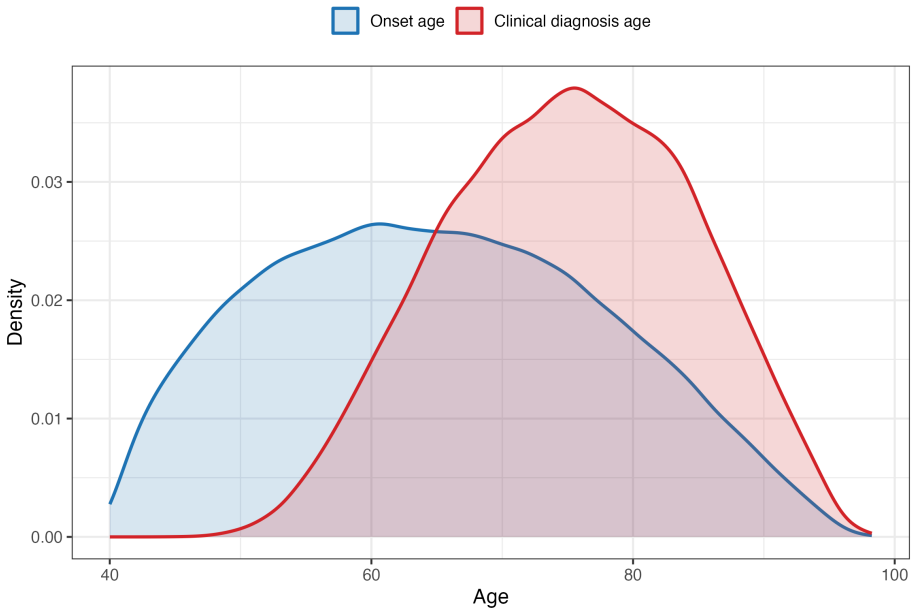

Screening and Detection

PSA screening occurs according to externally specified policies. Observed PSA values determine downstream decisions, including biopsy and additional testing. Secondary tests such as MRI are modeled as binary outcomes, with sensitivity depending on grade. Cancer detection through biopsy is modeled as a binary outcome, with sensitivity depending on grade.

Treatment

Initial treatment for prostate cancer is assigned based on disease characteristics at diagnosis (stage, grade, and mode of detection) under either idealized or population-based (realistic) treatment scenarios.

Under idealized treatment, individuals with localized or regional disease are assigned curative treatment (such as radical prostatectomy), while individuals with distant disease are assigned no curative treatment.

Under realistic treatment, individuals with localized or regional disease are assigned treatment according to empirical distributions (conservative management, radical prostatectomy, or radiotherapy) that depend on age at diagnosis, grade, and race. Conservative management is interpreted differently depending on disease characteristics: for screen-detected low-risk disease (localized, Gleason ≤6), it represents active surveillance,

whereas for higher-risk or regional disease it represents no curative treatment. Individuals with distant disease are not assigned curative treatment.

At the end of active surveillance, curative treatment (radical prostatectomy or radiotherapy) is assigned for individuals with localized or regional disease that are less than 85 years old.

Survival

Prostate cancer–specific survival is modeled using baseline survival functions that depend on age at diagnosis, stage, grade, and race, representing outcomes in the absence of screening and immediate curative treatment. These baseline survival functions can be adjusted to reflect contemporary management using a multiplicative transformation of the form:

$$S_0'(t) = S_0(t)^{\eta},$$

where $\eta < 1$ represents secular improvements in survival.

For individuals with localized or regional disease who receive curative treatment (radical prostatectomy or radiotherapy), survival is further modified according to:

$$S(t) = S_0'(t)^{0.55},$$

reflecting a constant hazard ratio associated with curative treatment. Individuals who do not receive curative treatment retain the baseline survival $S_0'(t)$.

For individuals diagnosed by screening with localized or regional disease, the benefit of early detection is modeled using a cure framework. A fraction of individuals are reassigned to die of other causes with probability:

$$1 - \exp(-\theta \ell),$$

where ℓ is the individual-specific lead time. For uncured individuals, survival follows the treated survival distribution. A similar cure mechanism is applied to individuals initially managed with active surveillance who subsequently receive curative treatment, with lead time defined relative to delayed treatment.

For individuals with distant disease at diagnosis or at the time of treatment assignment, survival follows the baseline distribution $S_0'(t)$, reflecting the absence of curative treatment.

Other-cause mortality is modeled independently using age- and cohort-specific life tables.

The cumulative incidence of prostate cancer mortality from time to diagnosis is presented in Figure 5.

Figure 5. Cumulative incidence of prostate cancer mortality from time of diagnosis by grade at diagnosis and treatment type.

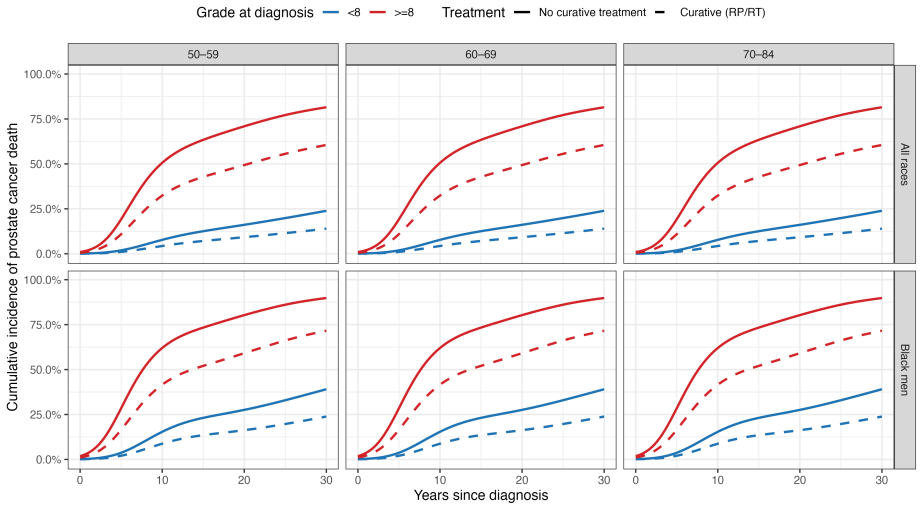

Active Surveillance

Active surveillance is assigned to individuals with screen-detected, low-risk prostate cancer (localized stage and Gleason ≤6) under realistic treatment scenarios. Surveillance consists of a confirmation biopsy approximately one year after diagnosis and subsequent biopsies every two years. The surveillance protocol approximates contemporary active surveillance practice patterns.

The duration of active surveillance is determined by the minimum of several competing times: time to clinical diagnosis under natural history, time to detection of upgrading under the surveillance protocol, time to transition to treatment (modeled using an exponential distribution with median 10 years), age 85, or death from other causes. Detection of upgrading is governed by the biopsy schedule and assumed sensitivity.

Individuals who exit active surveillance and remain eligible for curative treatment are assigned radical prostatectomy or radiotherapy based on treatment distributions conditional on receiving curative therapy. Individuals who progress to distant disease, reach age 85, or die from other causes are not assigned curative treatment.

Prostate cancer–specific survival for individuals managed with active surveillance is determined by their final treatment assignment and timing of treatment.

Parameter Overview

Parameter Overview

Summary

This document describes the parameters of the University of Michigan prostate cancer microsimulation model.

Background

Parameter values in the University of Michigan microsimulation model are informed by a combination of external data sources and calibration to population-level targets. External parameters, such as PSA dynamics and survival functions, are derived from clinical studies, observational datasets, or prior modeling work. Internal parameters governing tumor growth, disease progression, and detection are estimated through calibration to reproduce observed incidence patterns, stage and grade distributions at diagnosis, and survival outcomes consistent with the SCANS analytic model. This approach ensures that the microsimulation preserves consistency with established population-level evidence while allowing for modeling longitudinal processes.

Parameter Listing Overview

Parameters in the model are grouped by model component and identified as either internal (estimated via calibration) or external (specified from external data, assumptions, or prior analyses).

Tumor Onset (external)

- Weibull distribution scale and shape parameters (μ_O, s_O)

Tumor Growth (internal)

- Initial tumor extent at onset (R, fixed)
- Gamma distribution shape and rate parameters for tumor extent (α_E, θ_E)

PSA non-cancerous component (external)

- Mean and variance of the intercept of non-cancerous PSA component at age 35 (β_0, σ_0^2)
- Mean and variance of the slope of the non-cancerous PSA component (β_1, σ_1^2)
- PSA measurement error variance (σ_P^2)

PSA cancerous component (internal)

- Proportionality constant for cancer-related PSA component (δ)

Stage progression (internal)

- Stage transition hazard parameters for localized to regional and regional to distant stages (β_{1S}, β_{2S})
- Shape parameter for stage progression (s_S)

Grade progression (internal)

- Grade transition hazard parameters for Gleason score 2-6 to 7 and for Gleason score 7 to ≥8 (β_{1G}, β_{2G})
- Shape parameter for grade progression (s_G)

Clinical Detection (internal)

- Clinical detection scale and shape parameters (β_{CD}, s_{CD})

Screening and Biopsy (external)

- Screening policies (timing and frequency of PSA testing)
- MRI sensitivity (depends on grade and threshold)
- MRI specificity (depends on threshold)
- Biopsy sensitivity (depends on grade and biopsy method)
- Biopsy specificity (depends on biopsy method)

Treatment (external)

- Initial treatment assignment probabilities (depend on stage, grade, age)
- Hazard ratio for treatment effect

Prostate cancer specific survival (external)

- Baseline prostate cancer survival functions
- Secular improvement factor for survival
- Cure model parameter determining lead-time dependent cure

Other-cause mortality (external)

- Age- and cohort-specific mortality rates from life tables

Calibration

Model parameters governing progression, PSA dynamics, and disease characteristics at diagnosis were calibrated to multiple external and legacy data targets. Calibration was performed separately for all races combined and for Black men using a weighted objective function based on the root mean squared error (RMSE) between simulated and target quantities.

The calibration targets included:

(1) **Sojourn time distribution**
The distribution of time from latent onset to clinical diagnosis (sojourn time) was calibrated to race-specific survival curves estimated from the legacy University of Michigan SCANS model. Targets were stratified by age at onset (5-year groups from ages 40–85) and compared using simulated Kaplan–Meier survival functions for remaining free of clinical diagnosis following onset.

(2) **PSA distributions at onset and diagnosis**
PSA dynamics were calibrated using data derived from Fred Hutchinson Cancer Center (FHCC) cohorts. Calibration targets included:

- the distribution of PSA at latent onset stratified by age at onset, and
- the distribution of PSA at clinical diagnosis stratified by sojourn time.

PSA values were grouped into clinically relevant categories (0–10 ng/mL in 1-unit bins, followed by 10–15, 15–20, 20–30, and ≥30 ng/mL). Age at onset was categorized into 10-year age groups and sojourn time into 5-year intervals.

(3) **Stage and grade distributions at clinical diagnosis**
The joint distribution of stage and grade at clinical diagnosis was calibrated using FHCC and SCANS outputs. Disease stage was categorized as localized (L), regional (R), or distant (D), and Gleason grade groups were categorized as 2–6, 7, and 8–10. Calibration targets included:

- marginal grade distributions by age,
- marginal stage distributions by age, and
- joint stage-grade distributions by age.

Reduced stage-grade groupings combining localized/regional disease and lower Gleason categories (2–7 vs. 8–10) were additionally evaluated for consistency with SCANS outputs.

Calibration was performed using derivative-free numerical optimization. At each iteration, simulated life histories generated under the candidate parameter set were summarized into the same quantities as the calibration targets, and the overall objective function was computed as a weighted sum of RMSE values across calibration domains. Within individual calibration targets, discrepancies were weighted according to the observed frequency of outcome categories, placing greater emphasis on reproducing the most commonly observed patterns in the data. Additional diagnostic metrics, including multinomial deviance and Poisson deviance, were evaluated to assess goodness-of-fit.

Component Overview

Component Overview

Summary

This document describes the main components of the University of Michigan prostate cancer microsimulation model and how they interact to generate individual life histories and outcomes.

Overview

The University of Michigan microsimulation model consists of the following primary components:

- Demography and competing mortality
- Tumor onset and latent tumor growth
- PSA dynamics
- Disease progression and clinical diagnosis
- Screening and diagnostic pathways
- Treatment assignment and efficacy
- Prostate cancer survival

These components are integrated through a latent tumor growth process that links biological progression, biomarker evolution, and clinical events. Figure 1 provides a schematic of the microsimulation model natural history and clinical states.

Figure 1. Schematic representation of the SCOPE microsimulation model. Latent tumor extent drives PSA growth, disease progression, and clinical detection.

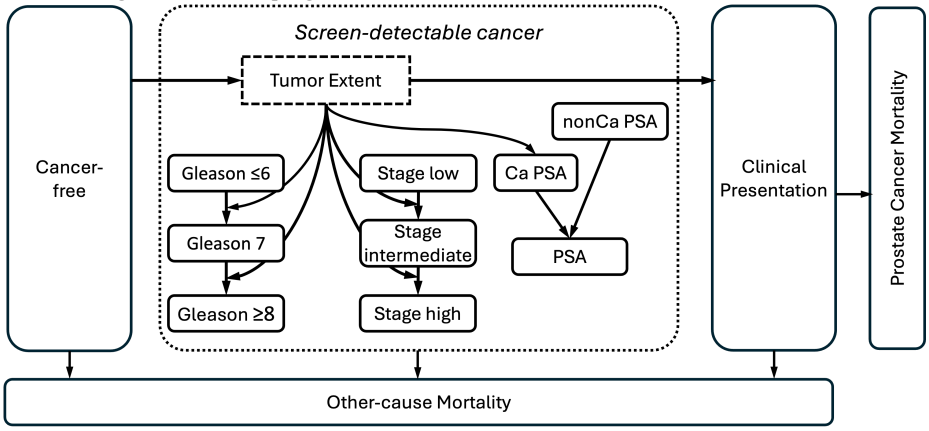

Component Listing

Demography and Competing Mortality

The demography component simulates individual life histories by assigning each individual a date of birth and an age at death from other causes based on population life tables. Other-cause mortality is modeled independently of prostate cancer and competes with all cancer-related events.

Tumor Onset and Latent Tumor Growth

The natural history component begins with the onset of preclinical prostate cancer, followed by progression governed by a latent tumor growth process. Tumor extent evolves over time according to an exponential growth model with subject-specific growth rates. This latent tumor extent is not directly observed but serves as the central driver of PSA dynamics, disease progression, and clinical detection.

PSA Dynamics

The PSA component generates longitudinal PSA measurements over time. PSA is modeled as the combination of a non-cancer component, which follows a linear trajectory on the log scale with age, and a cancer-related component that is proportional to tumor extent. This results in accelerated PSA growth following cancer onset. The PSA growth model is described in the Assumption Overview.

Disease Progression and Clinical Diagnosis

Disease progression is represented through transitions in stage (localized, regional, distant) and grade (2-6, 7, 8-10), both of which evolve as functions of tumor extent. Individuals begin in localized, low-grade disease at onset and may progress to more advanced stage and higher grade over time. Clinical diagnosis occurs according to a hazard function that depends on tumor extent and is calibrated to reproduce the sojourn time distribution from the SCANS model.

Screening and Diagnostic Pathways

Screening is superimposed on individual life histories and is applied according to specified policies. PSA measurements obtained at screening visits inform decisions regarding biopsy and additional diagnostic testing. Secondary tests, including MRI, are modeled with state-dependent sensitivity and specificity. Detection through biopsy is modeled as a binary outcome, with sensitivity depending on underlying disease characteristics (e.g., grade).

Screen detection may alter the timing of diagnosis and downstream clinical outcomes by advancing detection relative to clinical diagnosis.

Treatment

Following diagnosis, individuals are assigned treatment based on disease characteristics, including stage and grade, and may reflect either idealized or population-based treatment patterns. Treatment options include curative therapies or conservative management strategies such as active surveillance. Individuals with distant disease are not assigned curative treatment.

Prostate Cancer Survival

Survival following diagnosis is modeled using hazard functions that depend on age, stage, grade, and treatment. The benefit of screening is incorporated through a lead-time dependent cure mechanism, by which a fraction of screen-detected cases are reassigned to die from other causes. Prostate cancer–specific mortality competes with other-cause mortality to determine overall survival outcomes.

Output Overview

Output Overview

Summary

This document describes the main outputs of the University of Michigan prostate cancer microsimulation model.

Overview

The main outputs of the University of Michigan microsimulation model are:

- Individual life histories
- Aggregate outcomes
- Incidence data
- Mortality data
- Natural history summaries

Output Listing

Individual life histories

Simulated individual life histories track demographic, natural history, diagnostic, treatment, and survival events over time. A typical model run includes:

- Age at entry into the simulation
- Age at preclinical onset of prostate cancer
- Age at stage transitions
- Age at grade transitions
- Age at clinical diagnosis in the absence of screening
- Individual non-cancer PSA parameters
- Individual tumor growth parameters
- PSA level at onset
- PSA level at clinical diagnosis
- Stage at clinical diagnosis
- Grade at clinical diagnosis
- Primary treatment with screening (radical prostatectomy, radiotherapy, conservative management)
- Age at prostate cancer-specific death with screening
- Age at death from other causes

When screening is superimposed, simulated life histories may also include:

- Age at diagnosis with screening
- Mode of diagnosis (screen-detected or clinically detected)
- PSA at diagnosis with screening
- Stage at diagnosis with screening
- Grade at diagnosis with screening
- Treatment at diagnosis
- Age at prostate cancer death
- Cause of death

These individual life histories are written to output files for each simulated screening and treatment strategy and can be used to derive summary statistics such as overdiagnosis, lead time, sojourn time, and survival.

Overdiagnosis is defined as a screen-detected case that would not have been clinically diagnosed before death from other causes.

Overtreatment is defined as a screen-detected case that receives curative treatment that would not have been clinically diagnosed before death from other causes.

Lead time is defined as the time by which diagnosis is advanced under screening relative to clinical diagnosis in the absence of screening.

Sojourn time is defined as the time from preclinical onset to clinical diagnosis in the absence of screening.

Aggregate outcomes

The model records aggregate counts and person-time summaries for comparative effectiveness analyses. These outputs include:

- Total first-line screening (e.g., PSA) tests
- True positive first-line screening tests
- True negative first-line screening tests
- False positive first-line screening tests
- False negative first-line screening tests
- Total second-line screening (e.g., MRI) tests
- Total biopsies
- Screen-detected diagnoses
- Clinical diagnoses
- Overdiagnoses
- Overtreatments
- Radical prostatectomies
- Radiotherapy courses
- Active surveillance initiations
- Prostate cancer deaths
- Other-cause deaths
- Number alive without diagnosed prostate cancer
- Number with undiagnosed prostate cancer
- Life-years
- Life-years without diagnosed prostate cancer

These outputs may be tabulated by age and calendar year to support age-specific analyses, temporal trends, and policy comparisons.

Incidence data

Simulated prostate cancer incidence can be summarized using diagnosis counts and corresponding population denominators. These outputs may be tabulated by:

- Age at diagnosis
- Calendar year of diagnosis
- PSA at diagnosis
- Stage at diagnosis
- Grade at diagnosis
- Mode of detection

These summaries support comparison of projected incidence patterns under alternative screening and diagnostic strategies.

Mortality data

Simulated mortality outputs include both prostate cancer deaths and deaths from other causes, along with the corresponding population denominators needed to estimate rates. These outputs may be tabulated by:

- Age at death
- Calendar year of death
- PSA at diagnosis
- Stage at diagnosis
- Grade at diagnosis
- Mode of detection

These summaries support evaluation of prostate cancer mortality, competing mortality, and overall benefit–harm tradeoffs under alternative strategies.

Natural history summaries

Because the model explicitly simulates latent disease onset and progression, it also produces natural history summaries that are not directly observable in empirical data. These may include:

- Distribution of age at onset
- Distribution of sojourn times
- Distribution of tumor growth rates
- Time spent in undiagnosed preclinical disease
- Stage and grade distributions at different points in the natural history
- PSA values at onset and diagnosis

These outputs are useful for calibration, validation, and interpretation of how screening and treatment strategies interact with the underlying disease process.

Results Overview

Results Overview

Summary

This document summarizes selected results of the SCOPE model.

Validation

The microsimulation model was evaluated using both external population-level incidence data and trial-based screening outcomes to assess its ability to reproduce observed prostate cancer incidence and screening effects.

SEER incidence validation

Model validity was assessed by comparing simulated prostate cancer incidence patterns against age-, stage-, and grade-specific incidence rates from the Surveillance, Epidemiology, and End Results (SEER) program between 1975 and 2000. Validation was performed separately for all races combined and for Black men. Figure 1 compares age-specific incidence trends between simulated and observed SEER data and Figure 2 compares simulated and observed stage- and grade-specific incidence trends over calendar time. The model reproduced the major temporal trends in incidence, including the sharp PSA-era increase in localized disease and decline in distant-stage incidence.

Figure 1. Observed SEER and simulated prostate cancer incidence rates by age group and race, 1975–2000.

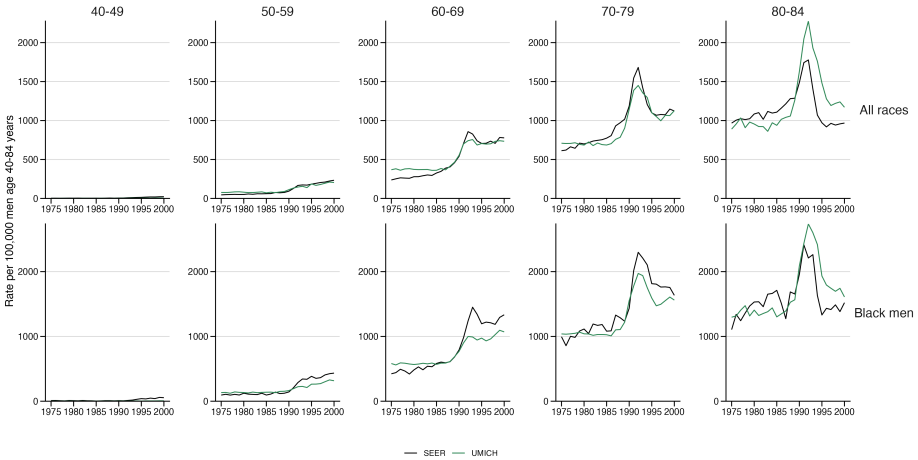

Figure 2. Observed SEER and simulated incidence rates by stage-grade category and race, 1975–2000.

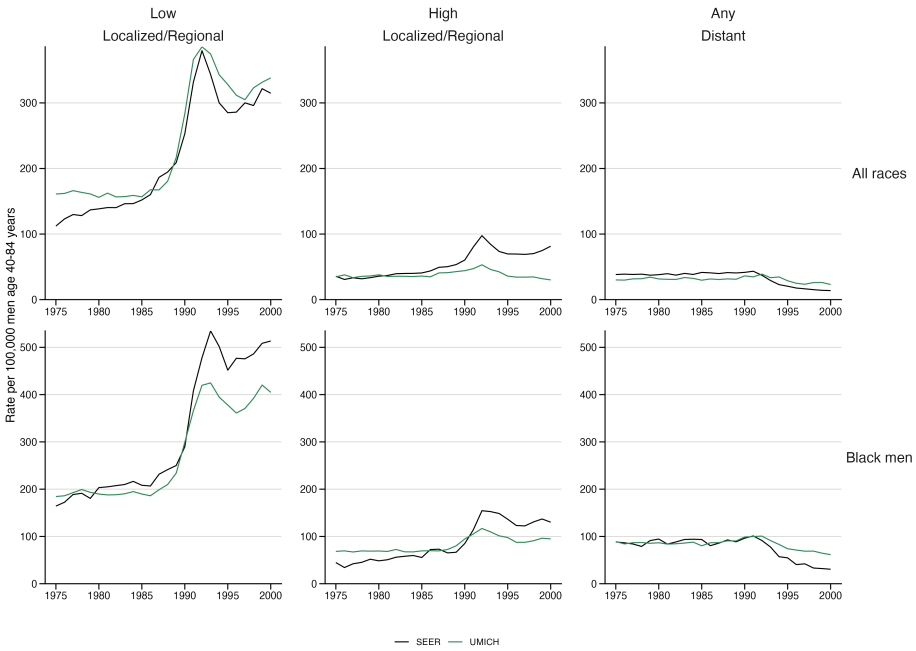

CAP trial validation

The model was evaluated by comparing simulated screening outcomes against results from the Cluster Randomized Trial of PSA Testing for Prostate Cancer (CAP). Simulated prostate cancer cumulative incidence over 20 years is presented for the intervention and control arms stratified by disease stage and Gleason grade in Figure 3. The model reproduced the expected increase in early-stage and lower-grade incidence in the intervention arm, with smaller differences for advanced and distant disease.

Figure 3. Simulated cumulative prostate cancer incidence in CAP-like screening and control arms stratified by stage and Gleason grade category over 20 years of follow-up.

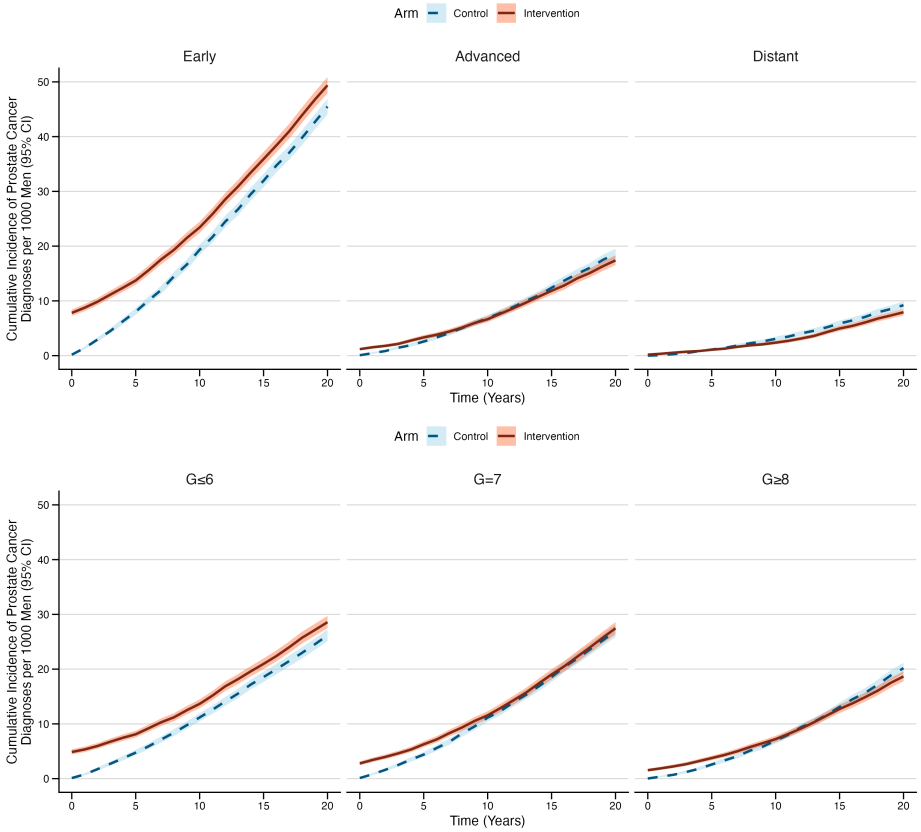

Comparison of Screening Strategies

We evaluated a large set of candidate prostate cancer screening strategies using the SCOPE microsimulation model. Simulations were performed separately for cohorts of U.S. general population men and U.S. Black men born in 1980 with no prior prostate cancer screening or personal history of prostate cancer.

A total of 180 candidate screening strategies were evaluated, varying according to screening start age (45, 50, or 55 years), stopping age (69 or 74 years), screening interval (1, 2, or 4 years), PSA threshold for biopsy referral (3 or 4 ng/mL), MRI confirmation pathway (PI-RADS threshold 3 or 4), biopsy approach (systematic biopsy, MRI-targeted biopsy, or combined MRI-targeted and systematic biopsy). Full adherence to PSA screening and confirmatory testing was assumed.

Figure 4 summarizes the tradeoff between screening benefits and harms across candidate strategies. The efficient frontier curves identify screening strategies that maximize prostate cancer deaths prevented for a given level of screening harm. Strategies below the frontier were dominated by alternative strategies that achieved greater mortality benefit with equal or lower biopsy burden or overdiagnosis. Benefits were quantified as prostate cancer deaths prevented relative to no screening, while harms were quantified using total biopsies and overdiagnoses per 1000 men. Across both racial groups, more intensive screening strategies generally produced larger reductions in prostate cancer mortality but also increased biopsy burden and overdiagnosis.

Strategies incorporating MRI-based confirmation pathways showed more favorable harm-benefit tradeoffs compared with strategies relying on systematic biopsy alone. In particular, MRI confirmation with a PI-RADS threshold of 4 achieved similar or greater reductions in prostate cancer mortality while requiring fewer biopsies and producing fewer overdiagnoses than less selective approaches. These improvements were observed in both the general population and Black men, although the absolute number of prostate cancer deaths prevented was consistently higher among Black men.

Figure 4. Tradeoffs between prostate cancer mortality benefit and screening harms across candidate screening strategies in the general U.S. population and Black men. Panels show prostate cancer deaths prevented relative to no screening versus total biopsies (left) and overdiagnoses (right) per 1000 men. Points represent individual candidate screening strategies stratified by confirmation pathway and biopsy approach, including systematic biopsy alone (TRUS only), MRI-targeted biopsy (MRGB), and combined MRI-targeted plus systematic biopsy (MRGB+TRUS) using PI-RADS thresholds of 3 or 4. Solid black curves represent the efficient frontier identifying non-dominated screening strategies.

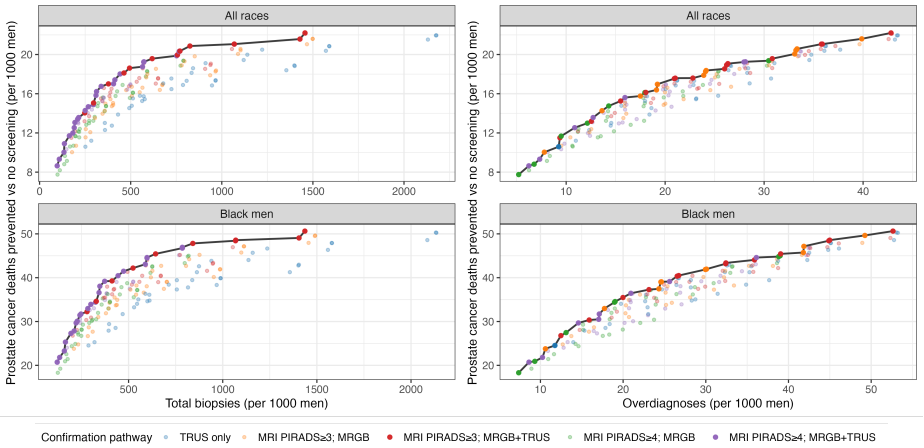

Key References

Chefo S, Tsodikov A. Stage-specific cancer incidence: An artificially mixed multinomial logit model. Statistics in medicine. Wiley Online Library; 2009;28(15):2054–2076.

Etzioni R, Tsodikov A, Mariotto A, Szabo A, Falcon S, Wegelin J, Ditommaso D, Karnofski K, Gulati R, Penson DF, others. Quantifying the role of PSA screening in the US prostate cancer mortality decline. Cancer Causes & Control. Springer; 2008;19(2):175–181.

Gulati R, Tsodikov A, Etzioni R, Hunter-Merrill RA, Gore JL, Mariotto AB, Cooperberg MR. Expected population impacts of discontinued prostate-specific antigen screening. Cancer. Wiley Online Library; 2014;120(22):3519–3526.

Tsodikov A, Szabo A, Wegelin J. A population model of prostate cancer incidence. Statistics in Medicine. Wiley Online Library; 2006;25(16):2846–2866.

Tsodikov A, Chefo S. Generalized self-consistency: Multinomial logit model and Poisson likelihood. Journal of statistical planning and inference. Elsevier; 2008;138(8):2380–2397.

Tsodikov A, Gulati R, Heijnsdijk EA, Pinsky PF, Moss SM, Qiu S, De Carvalho TM, Hugosson J, Berg CD, Auvinen A, others. Reconciling the effects of screening on prostate cancer mortality in the ERSPC and PLCO trials. Annals of internal medicine. American College of Physicians; 2017;167(7):449–455.

Tsodikov A, Gulati R, de Carvalho TM, Heijnsdijk EA, Hunter-Merrill RA, Mariotto AB, de Koning HJ, Etzioni R. Is prostate cancer different in black men? Answers from 3 natural history models. Cancer. Wiley Online Library; 2017;123(12):2312–2319.

Tsodikov A, Liu LX, Tseng C. Likelihood transformations and artificial mixtures. Statistical Modeling for Biological Systems: In Memory of Andrei Yakovlev. Springer; 2020. p. 191–209.

Wang S, Tsodikov A. A self-consistency approach to multinomial logit model with random effects. Journal of statistical planning and inference. Elsevier; 2010;140(7):1939–1947.

